APPLIED AND ENVIRONMENTAL MICROBIOLOGY, Apr. 2001, p. 1536–1541 Vol. 67, No. 4
0099-2240/01/$04.00+0 DOI: 10.1128/AEM.67.4.1536–1541.2001

Proline-Rich Peptide from the Coral Pathogen *Vibrio shiloi* That Inhibits Photosynthesis of Zooxanthellae

EHUD BANIN,[1] SANJAY K. KHARE,[2] FRED NAIDER,[2] AND EUGENE ROSENBERG[1]*

Department of Molecular Microbiology & Biotechnology, Tel Aviv University, Ramat Aviv, Israel 69978,[1] and Department of Chemistry, College of Staten Island, New York, and The Doctoral Program in Chemistry of the City University of New York, Staten Island, New York 10314[2]

Received 23 October 2000/Accepted 17 January 2001

The coral-bleaching bacterium *Vibrio shiloi* biosynthesizes and secretes an extracellular peptide, referred to as toxin P, which inhibits photosynthesis of coral symbiotic algae (zooxanthellae). Toxin P was produced during the stationary phase when the bacterium was grown on peptone or Casamino Acids media at 29°C. Glycerol inhibited the production of toxin P. Toxin P was purified to homogeneity, yielding the following 12-residue peptide: PYPVYAPPPVVP (molecular weight, 1,295.54). The structure of toxin P was confirmed by chemical synthesis. In the presence of 12.5 mM NH_4Cl, pure natural or synthetic toxin P (10 μM) caused a 64% decrease in the photosynthetic quantum yield of zooxanthellae within 5 min. The inhibition was proportional to the toxin P concentration. Toxin P bound avidly to zooxanthellae, such that subsequent addition of NH_4Cl resulted in rapid inhibition of photosynthesis. When zooxanthellae were incubated in the presence of NH_4Cl and toxin P, there was a rapid decrease in the pH (pH 7.8 to 7.2) of the bulk liquid, suggesting that toxin P facilitates transport of NH_3 into the cell. It is known that uptake of NH_3 into cells can destroy the pH gradient and block photosynthesis. This mode of action of toxin P can help explain the mechanism of coral bleaching by *V. shiloi*.

Coral bleaching is the disruption of the symbiotic association between coral hosts and their photosynthetic microalgal endosymbionts, referred to as zooxanthellae (12). Coral bleaching events of unprecedented frequency and global extent have been reported during the last two decades (13). It has been suggested that coral bleaching is triggered by environmental factors which impose stress on the coral. The most frequently reported stress condition is increased seawater temperature (5, 16). Thus, it is possible that global warming could result in alteration or destruction of coral reef systems. Consequently, it is essential to understand the mechanism(s) of coral bleaching.

Bleaching of the coral *Oculina patagonica* from the Mediterranean Sea is the result of a bacterial infection (17, 18). The causative agent, *Vibrio shiloi*, was obtained in pure culture and was shown to cause bleaching in controlled aquarium experiments. Furthermore, it was shown that bacterium-induced bleaching by *V. shiloi* could be inhibited by antibiotics. The bacterial infection and resulting coral bleaching were temperature dependent, occurring only at elevated seawater temperatures (25 to 30°C).

Using the *V. shiloi-O. patagonica* model system to study coral bleaching, Toren et al. demonstrated that the first step in the infectious process was adhesion of *V. shiloi* to a β-galactoside-containing receptor on the coral surface (32). After *V. shiloi* adheres to *O. patagonica*, it penetrates into the exodermal layer of the coral (2). However, the mechanism by which the bacterium kills the algae is unknown. Recently, we reported that *V. shiloi* secretes extracellular materials that inhibit photosynthesis and bleach and lyse zooxanthellae isolated from corals (4). The material responsible for inhibition of photosynthesis was heat stable and was produced only when the bacteria were grown at elevated seawater temperatures.

In the present paper we describe production, purification, and characterization of a proline-rich dodecapeptide from *V. shiloi* that rapidly inhibits photosynthesis of zooxanthellae in the presence of NH_3.

MATERIALS AND METHODS

Bacterial strain and growth conditions. *V. shiloi* AK1 (= ATCC BAA-91), isolated from bleached coral as previously described (6), was used in this study. The strain was maintained on MB agar (1.8% marine broth [Difco] plus 0.9% NaCl solidified with 1.8% agar). After streaking, the plates were incubated at 30°C for 2 days and then allowed to stand for 1 week. For experiments described here, the bacteria were grown in MBT medium (1.8% marine broth, 0.75% tryptone, 0.9% NaCl), CA medium (0.75% Casamino Acids, 2% NaCl), and CAG medium (0.5% Casamino Acids, 0.5% glycerol, 2% NaCl) at 29°C with shaking.

Preparation of zooxanthellae from coral. Intact colonies of the coral *O. patagonica* were collected from a depth of 1 to 3 m along the Mediterranean coast of Israel. Within 2 h of collection, each colony was split into several pieces, and the pieces were placed into 2-liter aerated aquaria containing filtered (pore size, 0.45 μm) seawater that were maintained at 25°C. The aquaria were illuminated with a fluorescent lamp by using cycles consisting of 12 h of light and 12 h of darkness. To obtain zooxanthellae, a healthy coral fragment (surface area, ~1 cm^2) was removed from an aquarium and rinsed gently with filter-sterilized seawater, and then the tissue was disrupted with a dental water pick by using ca. 50 ml of sterile seawater. The suspension was centrifuged for 30 min at 2,000 × *g*. The pellet, resuspended in 1 ml of seawater, was then centrifuged in an Eppendorf centrifuge (model 5402) for 4 min at 10,000 rpm. The pellet, resuspended in 1 ml of seawater, was then centrifuged for 21 min at 1,200 rpm. The final pellet was resuspended in seawater to a concentration of ca. 5×10^6 algae per ml (based on hemacytometer counts). Fresh zooxanthella preparations were used in all experiments.

Purification of toxin P. Cultures of *V. shiloi*, grown in MBT medium for 72 h at 29°C, were centrifuged at 12,000 × *g* for 10 min at 4°C. The supernatant fluid was then passed through a 0.2-μm-pore-size Millipore membrane filter. Ammo-

* Corresponding author. Mailing address: Department of Molecular Microbiology & Biotechnology, Tel Aviv University, Ramat Aviv, Israel 69978. Phone: 972-3-640 9838. Fax: 972-3-642 9377. E-mail: eueqene@ccsg.tau.ac.il.

nium sulfate was added with stirring at 0°C to the cell-free supernatant fluid to a final concentration of 80% saturation. After the preparation stood overnight at 4°C, the precipitate was collected by centrifugation and dissolved in 1/10th the initial volume of water. The concentrated crude toxin P was then extracted three times with an equal volume of ethyl acetate. The ethyl acetate extracts were combined and evaporated to dryness in vacuo at 30°C.

Three sequential columns were used to purify the peptide. The ethyl acetate-extracted material was dissolved in 1 ml of 50 mM Tris HCl buffer (pH 8.0) and applied to a Resource Q column (Pharmacia Bio Tech) with a bed volume of 1 ml and a height of 30 mm. The column was developed with a 0 to 1 M NaCl gradient at a flow rate of 1 ml/min. The active fractions (unconcentrated) were then run on a Superdex Peptide HR 10/30 column (bed volume, 24 ml; particle size, 13 μm; Pharmacia) and eluted with 50% ethanol at a flow rate of 0.25 ml/min. The active fractions were concentrated by evaporation in vacuo. The final purification was on an RP18 hydrophobic column (Merck) at a flow rate of 1 ml/min using increasing acetonitrile (ACN) concentrations.

Measurement of photosynthetic quantum yield of zooxanthellae. A portable underwater mini pulse-amplitude-modulation fluorometer (Walz) was used to measure the quantum yield of zooxanthellae. This instrument allows direct non-invasive measurement of the effective quantum yield of photosystem II under ambient light conditions (15, 23–25). Good correlations between measurements of quantum yield and photosynthetic rates (determined by O_2 evolution and CO_2 uptake) have been reported for plants (10) and cyanobacterial symbionts of lichens (31).

In the experimental procedure used here, the quantum yield of 0.05 ml of zooxanthellae in seawater (5×10^6 algae per ml) was measured in an enzyme-linked immunosorbent assay plate (Y_0). Measurements were obtained in the presence of a fluorescent lamp (light intensity, 16 μmol of photons m^{-2} s^{-1}) at 25°C. Then 0.05 ml of sterile seawater, 0.05 ml of growth medium (controls), or 0.05 ml of an experimental sample was added to the algae, and the kinetics of the quantum yield (Y_t) were measured with the mini pulse-amplitude-modulation fluorometer from 1 to 60 min. The percent quantum yields at different times were determined as follows: $Y_t/Y_0 \times 100$.

Determination of toxin P activity. In the initial growth experiments, toxin P activity was determined by removing a sample from a culture, centrifuging it to remove the cells, extracting the supernatant fluid with ethyl acetate three times, evaporating the combined ethyl acetate extracts to dryness in vacuo, and dissolving the residue in 50% ethanol. Dilutions of the solution (in sterile seawater) were then used to measure inhibition of photosynthesis of zooxanthellae in the presence of 12.5 mM NH_4Cl (unless stated otherwise), as described above. Inhibition due to NH_4Cl alone and ethyl acetate-extracted media (controls) was subtracted before toxin P activity was calculated. One unit of toxin P activity was defined as a 10% decrease in the quantum yield after 10 min of incubation. The same procedure was used for assaying purified toxin P except that the ethyl acetate step was omitted.

Micro sequence analysis. Automated Edman degradation of the purified peptide was performed with pulse liquid automatic sequentor (Applied Biosystems model 473A) by Technion Protein Laboratory, Haifa, Israel.

Solid-phase peptide synthesis of toxin (PYPVYAPPPVVP). Val-to-Val couplings are often sluggish, and Pro at the carboxyl terminus of a peptide has been associated with high levels of diketopiperazine formation during solid-phase peptide synthesis (28). Given the fact that the peptide toxin had a Val-Val-Pro sequence at the carboxyl terminus, a synthetic strategy that would minimize diketopiperazine formation during the Val-Val coupling step was developed. Accordingly, synthesis was carried out on a 2-chlorotrityl chloride resin because the bulk of the trityl handle minimized diketopiperazine formation during tripeptide formation. The tripeptide 9-fluorenylmethoxy-carbonyl (Fmoc)–Val–Val–Pro–Resin was synthesized manually, and after evaluation of its quality, chain assembly was completed by using an Applied Biosystems synthesizer.

The protected tripeptide was assembled by manual solid-phase synthesis, starting with H–Pro–2-chlorotrityl chloride resin (0.52 mmol/g). Coupling of Fmoc-Val was accomplished by using the bromo-tris-pyrrolidino-phosphonium hexafluorophosphate–diisopropylethyl amine procedure (8). Double coupling was carried out at both the di- and tripeptide stages to avoid deletion sequences. Complete coupling was confirmed by using the Kaiser test (14). A small portion of Fmoc-Val-Val-Pro-resin was cleaved by using a trifluoroacetic acid (TFA)-triisopropylsilane-H_2O cocktail (95:2.5:2.5, vol/vol/vol) to assess the purity of the peptide. High-performance liquid chromatography (HPLC) analysis indicated that the purity of the crude tripeptide was more than 95%. This product was judged acceptable for completion of synthesis.

Chain assembly from Fmoc-Val-Val-Pro-trityl resin was continued in a stepwise manner on a 0.1-mmol scale by using an Applied Biosystems, Inc., model 433A synthesizer. The coupling protocol used was the FastMoc chemistry protocol using 2-(1-H-benzotriazol-lyl)-1,1,3,3-tetramethyluronium hexafluorophosphate–1-hydroxytriazole activation. The Fmocgroup was used for protection of all N-α groups except the N-terminal group, where Boc-Pro was used. Tert-butyl was employed for protection of the Tyr side chain. All Fmoc groups were deprotected in 20% piperidine in *N*-methylpyrrolidine. After chain assembly was completed, the protected peptidyl resin was treated with TFA-triisopropylsilane-water (95:2.5:2.5, vol/vol/vol) at room temperature for 1.5 h. The reaction mixture was filtered to remove the resin, the resin was washed with TFA, and the combined filtrates were concentrated to a small volume with a rotary evaporator. The crude peptide obtained in this way was precipitated with cold diethyl ether.

The crude peptide was purified on a Waters μBondpack semipreparative C_{18} column (19 by 300 mm). A water-ACN-TFA gradient was used. The purity of the final product was assessed by using analytical reversed-phase HPLC (Hewlett-Packard series 1050 or 1090 HPLC) with a Waters μBondpack C_{18} column (3.9 by 300 mm), water-ACN-TFA and water-methanol-TFA elution systems, and detection at 220 and 260 nm. Homogeneity was also assessed by silica gel thin-layer chromatography (Silica Gel 60 precoated aluminum sheet from E. Merck, Darmstadt, Germany) with a gel developed in *n*-butanol–acetic acid–water–pyridene(9:2:4:3) and *n*-butanol–acetic acid–water (2:1:1); iodine was used as the developer. Electron spray ionization mass spectrometry was performed at PeptidoGenic Research Company, Livermore, Calif.

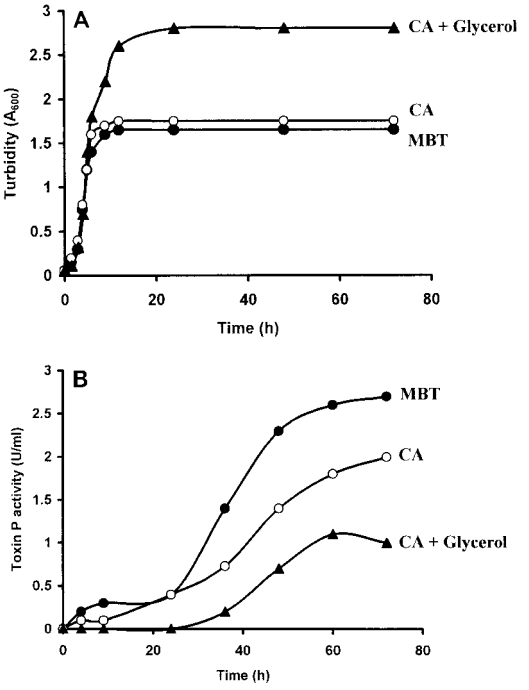

FIG. 1. Kinetics of growth and toxin P production in different media. An overnight culture of *V. shiloi* was inoculated into MBT (●), CA (○), and CAG (▲) media and incubated with shaking at 29°C. At intervals samples were removed for determinations of growth turbidity (A) and toxin P activity (B) as described in Materials and Methods.

RESULTS

Growth and toxin P production. *V. shiloi* grew exponentially with approximately the same doubling times (40 min) in MBT, CA, and CAG media, reaching final cell turbidities (A_{600}) of 1.7, 1.8, and 2.8, respectively (Fig. 1A). Extracellular photosynthetic inhibitor (toxin P) activity appeared after growth ceased and increased during the stationary phase (Fig. 1B). Although MBT medium supported the lowest cell yield, it yielded the highest toxin P activity (2.6 U/ml). Addition of glycerol to Casamino Acids medium (CAG medium) increased the cell yield but both delayed and inhibited toxin P produc-

TABLE 1. Purification of toxin P

Purification step	Toxin P activity (u)[b]	A_{210} (u)[c]	Sp act (U/A_{210} unit)	Yield (%)
Cell-free culture[a]	2,500			100
Ammonium sulfate	1,700	305	5.6	68
Ethyl acetate extraction	1,350	120	11	54
RQ column	1,100	70	16	44
Superdex peptide column	950	44	21.5	38
Hydrophobic column	650	3.3	197	26

[a] One liter of cell-free culture fluid from a *V. shiloi* culture grown for 72 h at 29°C in MBT medium was used to purify toxin P.
[b] Toxin P activity was measured by measuring inhibition of zooxanthella photosynthesis as described in Materials and Methods.
[c] After each purification step, the A_{210} was determined and multiplied by the volume to obtain the total number of absorbance units.

tion. The small amount of toxin P activity that was produced appeared only after the glycerol had been depleted from the medium. Furthermore, in glycerol-salts medium, *V. shiloi* grew to a final turbity (A_{600}) of 1.85 but produced no toxin P activity. Thus, glycerol, which is an excellent carbon source for growth of *V. shiloi*, inhibits toxin P production. Ethyl acetate extraction of cells from exponential- and stationary-phase cultures in MBT, CA, and CAG media resulted in only traces of toxin P activity, indicating that the cells did not accumulate the toxin (data not shown).

Purification of toxin P. Toxin P was purified to homogeneity by five purification steps (Table 1). Precipitation with an 80% $(NH_4)_2SO_4$ solution, followed by ethyl acetate extraction, concentrated and partially purified the activity. When a cation-exchange (RQ) column was used, all of the activity that was recovered eluted as a single peak in the flowthrough volume. Toxin P activity eluted as a single peak with an apparent molecular weight of approximately 14,000 as determined by gel filtration (Fig. 2A). In the final purification step, in which a hydrophobic column was used, the activity eluted as a symmetrical peak at 35% ACN (Fig. 2B). The overall yield was 26%, and the toxin was purified 35-fold from the ammonium sulfate fraction to the final product. HPLC and thin-layer chromatography demonstrated that the product was more than 95% pure.

Chemical properties of toxin P. Pure toxin P was subjected to Edman degradation, which gave the following 12-residue sequence: PYPVYAPPPVVP. This sequence fits precisely the molecular mass of 1,295.54 Da determined by mass spectroscopy. Thus, toxin P is a linear, proline-rich dodecapeptide. The calculated pI is 5.99. Toxin P had an absorbance maximum at 275 nm at pH 7.0, and a molecular extinction coefficient of 2,800, which is typical of a peptide with two tyrosine residues.

To verify the structure and further investigate the mode of action, the putative 12-residue toxic peptide was synthesized by using a solid-phase strategy on a chlrotrityl resin to avoid diketopiperazine formation during formation of the tripeptide. The final crude product was nearly 90% homogeneous and was readily purified almost to homogeneity as judged by both HPLC and thin-layer chromatography with two different solvent systems. The overall yield of the synthesis procedure, including the assembly, cleavage, and purification steps, was 20%. The molecular mass of the product was within 1 Da of the calculated value. The specific photosynthesis inhibitor activity of the synthetic peptide (4.6 U/μg) was similar to that of

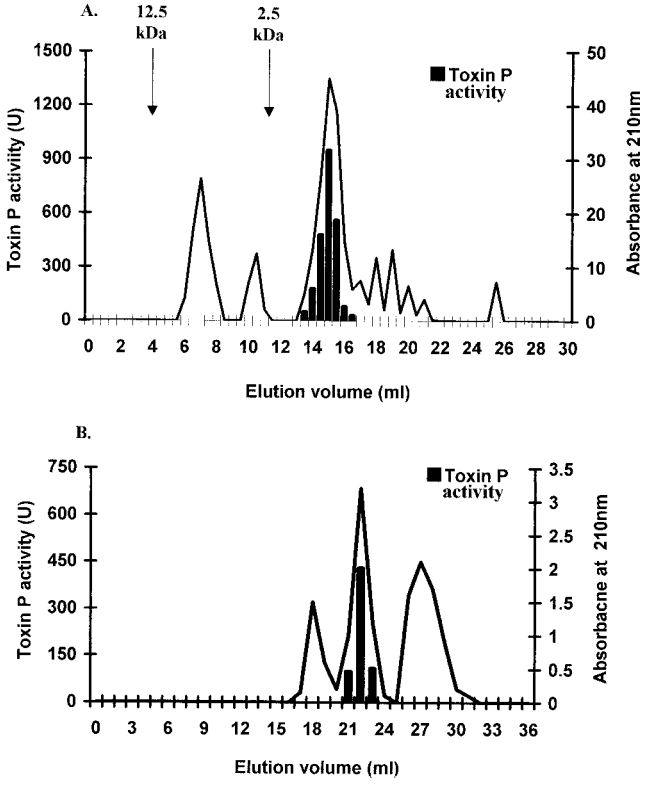

FIG. 2. Chromatographic purification of toxin P. (A) Partially purified toxin P was applied to a Superdex Peptide HR 10/30 (gel filtration) column and eluted with 50% ethanol. The arrows indicate the elution volumes of standard molecular weight markers. (B) The active fractions from the gel filtration column (14 to 16 ml) were concentrated, applied to an RP18 hydrophobic column, and eluted with increasing ACN concentrations.

pure natural toxin P (5.0 U/μg). The properties of the synthetic material confirmed the structure of the toxin isolated and supported the hypothesis that this peptide is the biologically active agent.

When natural toxin P was eluted on a gel filtration column in the presence of 50% ethanol, it eluted as a sharp peak with an apparent molecular weight of 1,300 (Fig. 3). However, when the toxin was eluted in the absence of ethanol, it gave a broad

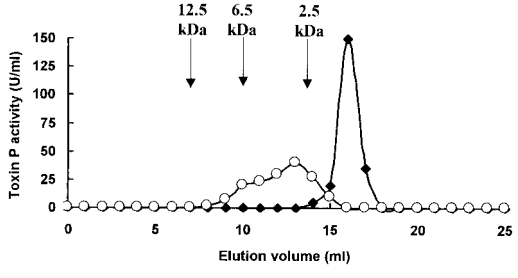

FIG. 3. Gel filtration of toxin P in 50% ethanol (●) and 50 mM Tris-HCl buffer (pH 8.0) (○). Purified toxin P was eluted on a Superdex Peptide HR 10/30 column, and fractions were analyzed for photosynthesis-inhibiting activity as described in Materials and Methods. The arrows indicate the positions of elution of standard molecular weight markers.

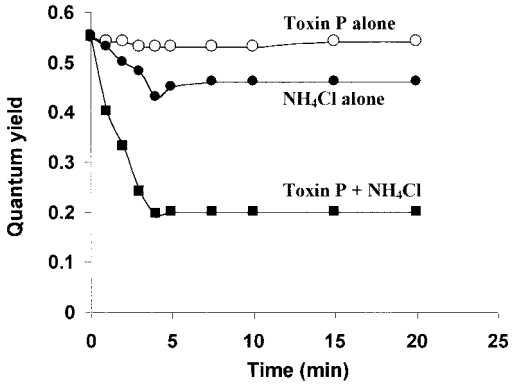

FIG. 4. Kinetics of inhibition of algal photosynthesis by toxin P. The photosynthetic quantum yield of fresh zooxanthellae was measured in seawater containing 20 mM Tris-HCl buffer (pH 8.0) and 10 μM toxin P (○), 12.5 mM NH_4Cl (●), or 10 μM toxin P plus 12.5 mM NH_4Cl (■). A control containing zooxanthellae in seawater and buffer gave the same data as toxin P alone.

TABLE 2. Binding of toxin P to zooxanthellae[a]

Treatment	Quantum yield		
	Initial treatment	After algae were washed	After addition of NH_4Cl to washed algae[b]
Seawater control	0.59	0.60	0.52 (13)
NH_4Cl	0.54	0.60	0.51 (15)
Toxin P	0.60	0.60	0.31 (48)
Toxin P + NH_4Cl	0.20	0.27	0.10 (83)

[a] Tubes containing zooxanthellae in seawater were treated with 10 mM NH_4Cl, 10 μM toxin P, or a mixture of NH_4Cl and toxin P. Algae in seawater served as a control. After 10 min of incubation, the photosynthetic quantum yield was determined (initial treatment). The tubes were then centrifuged at 1,000 × *g* for 10 min. After the supernatant fluid was removed, the algal pellets were suspended in seawater, and the centrifugation step was repeated. After incubation of the algae for 1 h in the presence of light, the quantum yield was again determined. Finally, 10 mM NH_4Cl was added to each of the tubes, and the quantum yield was determined.

[b] The numbers in parentheses are the percentages of inhibition of quantum yield after addition of NH_4Cl to the washed algae.

peak with an apparent molecular weight of ca. 2,500 to more than 7,000. Thus, in aqueous solutions, toxin P appears to aggregate.

Inhibition of algal photosynthesis by toxin P. In the presence of NH_4Cl, natural toxin P rapidly inhibited photosynthesis of zooxanthellae (Fig. 4). One minute after addition of the toxin and NH_4Cl to the algae, the photosynthetic quantum yield decreased 27%, from 0.55 to 0.40. Inhibition became progressively stronger for the next 3 min and then leveled off at 64%. Under the same conditions, NH_4Cl by itself inhibited the quantum yield by 18% after 5 min, and then the quantum yield remained constant. Similar results were obtained with the synthetic toxin P. In the absence of NH_4Cl, toxin P had no effect on algal photosynthesis.

The effect of the synthetic toxin P concentration on quantum yield is shown in Fig. 5. The inhibition was linear with toxin P concentrations from 2.5 to 10 μM, with a slope of 6% per μM. In this linear range, 1 U of toxin P activity (defined as the activity which resulted in a 10% decrease in quantum yield) was obtained per 1.7 μM, which corresponded to 0.22 μg of toxin P in a 0.1-ml assay tube. At toxin P concentrations less than 2.5 μM, the inhibition was less than that predicted from the linear relationship, suggesting that there may be a minimum concentration necessary to affect inhibition of photosynthesis.

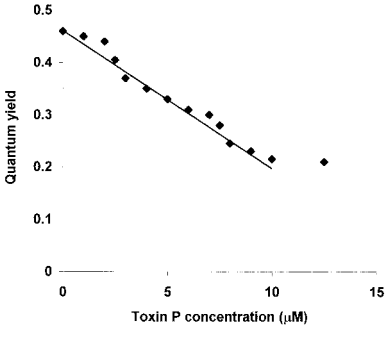

FIG. 5. Inhibition of algal photosynthesis as a function of toxin P concentration. The experiment was performed as described in Materials and Methods by using 12.5 mM NH_4Cl and different concentrations of the chemically synthesized peptide. The quantum yield was recorded after 10 min of incubation.

Binding of toxin P to zooxanthellae. To test if the effect of toxin P and NH_4Cl on zooxanthella photosynthesis was reversible, algae were washed extensively after different treatments. The quantum yields of the washed algae were then measured before and after addition of NH_4Cl (Table 2). The algae in the seawater control maintained a high photosynthetic quantum yield (0.60) after the washing treatment. Addition of 10 mM NH_4Cl to the washed control resulted in a 13% decrease in the quantum yield. Algae that were initially treated with NH_4Cl completely recovered their quantum yield after the washing procedure and showed a 15% decrease after a second addition of NH_4Cl. Interesting data were obtained with the algae treated initially with toxin P and toxin P plus NH_4Cl. As expected (from the data presented in Fig. 4), toxin P alone had no effect on quantum yield, whereas toxin P plus NH_4Cl resulted in 67% inhibition. Algae treated with toxin P and then washed extensively in seawater retained all of their photosynthetic activity, but when they were treated with NH_4Cl, they showed a 48% decrease in quantum yield. Thus, toxin P remained bound to the algal cells and subsequently exhibited its synergistic effect with NH_4Cl. Algae treated initially with both toxin P and NH_4Cl recovered photosynthesis efficiency only partially after washing. Addition of NH_4Cl to the washed cells led to strong inhibition of the quantum yield (83%), again indicating that toxin P remained bound to the zooxanthellae. The experiments described above were preformed with both natural toxin P and synthetic toxin P, which yielded identical data.

Toxin P-induced pH changes. When cells take up NH_3 more rapidly than NH_4^+, the pH of the bulk liquid decreases as a result of dissociation of NH_4^+ to NH_3 and H^+. To test the hypothesis that toxin P catalyzes movement of NH_3 into zooxanthellae, pH changes were monitored in algal suspensions containing NH_4Cl and NH_4Cl plus natural toxin P (Fig. 6). The pH of algae in unbuffered seawater remained constant at 7.8. Addition of 15 mM NH_4Cl caused the pH to drop to 7.6 in 5

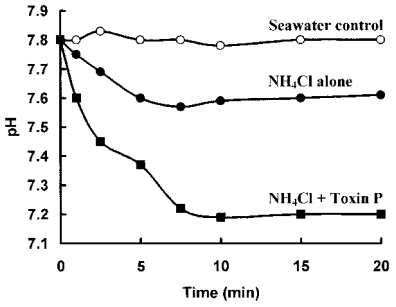

FIG. 6. Toxin P-induced pH changes. To 1 ml of zooxanthellae (5×10^6 cells/ml) in unbuffered seawater 15 mM NH_4Cl (●) or 10 μM toxin P plus 15 mM NH_4Cl (■) was added. At intervals the pH of the suspension was measured. Algae in seawater served as a control (○).

min, and then the pH remained constant. Toxin P by itself had no effect on the pH (data not shown). However, addition of toxin P plus 15 mM NH_4Cl resulted in a large, rapid decrease in the pH, which reached 7.45 after 2 min and 7.2 after 7 min. Thus, toxin P facilitated transport of NH_3 into the algae. Titration of 15 mM NH_4Cl in seawater from pH 7.8 to 7.2 required 1.7 mM HCl. Thus, ca. 1.7 mM NH_3 (the equivalent amount of NH_4^+ converting to NH_3 plus H^+) must have entered the algae. Accordingly, each toxin molecule (concentration in the experiment, 10 μM) must have been responsible for transport of ca. 170 molecules of NH_3.

DISCUSSION

The data presented here demonstrate that toxin P is a linear, proline-rich dodecapeptide. It is likely that toxin P is produced from a larger peptide by proteolysis. The amino acid sequence of toxin P shows strong similarity (10 of the 12 amino acids are identical) to the amino acid sequence of an internal peptide in the *vrg-6* gene product of *Bordetella pertussis* (GenBank accession number M77374). It has been suggested that the *vrg* gene products facilitate intracellular survival and the persistence of the bacterium in the host (3). In this regard it is interesting that *V. shiloi* is also an intracellular pathogen (2).

The high hydrophobicity predicted from the amino acid sequence of toxin P may help explain the observed binding of the toxin to zooxanthellae. Bound toxin P by itself did not affect algal photosynthesis. However, addition of NH_4Cl to algae containing the bound toxin resulted in rapid inhibition of photosynthesis and a concurrent decrease in the pH of the bulk liquid. Inhibition of photosynthesis by ammonia is well established (1, 7, 35). Ammonia acts as an uncoupler of photosynthesis by passing across membranes, thereby destroying the pH gradient across the thylakoid membrane (27, 34). Many membrane-penetrating peptides, including melittin (33), gaegurin (29), cecropin (22), and buforin (21), contain prolyl residues. Although the exact role of prolyl in the function of these peptides is unknown, proline causes kinks in helical polypeptides and increases the flexibility of peptide chains in its immediate environment. Some of these peptides cause lysis of cell membranes, while others act as ion channel formers (30). In addition, some membrane-active peptides orient parallel to the bilayer, whereas others orient perpendicular to the plane of the membrane (26). Very recently, a hydrophilic proline-rich domain from the C terminus of L-type calcium channels was shown to remain membrane associated (11). Cyclic peptides rich in proline have been found to bind alkali metals (9, 19). Since toxin P is a dodecapeptide, it cannot traverse the membrane bilayer. However, it could form aggregates of the head-to-head or head-to-tail type, as found for gramicidin A. Furthermore, toxin P aggregates in aqueous solution (Fig. 3), supporting the hypothesis that it can enter the algal membrane and act as an ammonia channel. However, the possibility that ammonia activates toxin P has not been eliminated.

Proline-rich antibacterial peptides are also produced by mammalian neutrophils (20). These peptides are mainly active against gram-negative bacteria. Investigation of the secondary structure of one of these peptides (PR-39), which contains 39 amino acids (19 Pro residues), suggests that it exists in a polyproline II conformation in water. After interacting with the membrane, PR-39 rapidly enters human microvascular endothelial cells and binds to a number of cytoplasmic proteins (6). Now that pure chemically synthesized toxin P is available, it should be possible to examine its structure and mode of action in more detail. It will also be interesting to examine synthetic peptides with defined amino acid replacements in order to determine their ability to inhibit photosynthesis.

In considering the natural role of toxin P in pathogenesis (coral bleaching), we should mention that high levels of toxin P were found in coral tissues shortly after infection with *V. shiloi* (8). The toxin is produced only at the elevated seawater temperatures (25 to 30°C) necessary for bacterial bleaching of corals (16). Presumably, once *V. shiloi* penetrates into the coral tissue, it produces toxin P and ammonia (from metabolism of coral cytoplasmic protein). The resulting inhibition of photosynthesis in the intracellular zooxanthellae would damage the algae and contribute to coral bleaching (loss of the algae). It should be noted that the equilibrium of NH_4^+ dissociation to NH_3 is shifted towards increased NH_3 formation with increasing temperature. For example, three times more NH_3 is produced at 25°C than at 10°C at a constant pH and a constant total NH_3-NH_4^+ concentration. It should be noted that *O. patagonica* in the eastern Mediterranean Sea experiences a shift in temperature from 16°C (winter) to 29 to 30°C (summer, when bleaching occurs) (16). This may contribute to magnification of the toxin P-enhanced toxicity of ammonia for zooxanthellae in infected coral during the summer.

ACKNOWLEDGMENTS

This work was supported by United States-Israel Binational Science Foundation grant 95-00177, by the Pasha Gol Chair for Applied Microbiology, by the Israel Center for the Study of Emerging Diseases, and by National Institutes of Health grant GM 22086 to F. Naider.

F. Naider is currently a Varon Visiting Professor at the Weizmann Institute of Science, Rehovot, Israel. We thank G. Fleminger for help with the HPLC analysis.

REFERENCES

1. **Abeliovich, A., and Y. Azov.** 1976. Toxicity of ammonia to algae in sewage oxidation ponds. Appl. Environ. Microbiol. **31:**801–806.
2. **Banin, E., T. Israely, A. Kushmaro, Y. Loya, E. Orr, and E. Rosenberg.** 2000. Penetration of the coral-bleaching bacterium *Vibrio shiloi* into *Oculina patagonica*. Appl. Environ. Microbiol. **66:**3031–3036.
3. **Beattie, D. T., R. Shahin, and J. J. Mekalanos.** 1992. A vir-repressed gene of *Bordetella pertussis* is required for virulence. Infect. Immun. **60:**571–577.
4. **Ben-Haim, Y., E. Banin, A. Kushmaro, Y. Loya, and E. Rosenberg.** 1999. Inhibition of photosynthesis and bleaching of zooxanthellae by the coral

pathogen *Vibrio shiloi*. Environ. Microbiol. **1:**223–229.
5. **Brown, B. C.** 1997. Coral bleaching: causes and consequences, p. 65–74. *In* Proceedings of the 8th International Coral Reef Symposium, Vol. 1. Smithsonian Tropical Research Institute, Balboa, Panama.
6. **Cabiaux, V., B. Agerberth, J. Johansson, F. Homble, E. Goormaghtigh, and J. M. Ruysschaert.** 1994. Secondary structure and membrane interaction of PR-39, a Pro + Arg-rich antimicrobial peptide. Eur. J. Biochem. **24:**1019–1027.
7. **Cohen, D. E., W. S. Cohen, and W. Bertsch.** 1975. Inhibition of photosystem II by uncouplers at alkaline pH and its reversal by artificial electron donors. Biochim. Biophys. Acta **376:**97–104.
8. **Coste, J., E. Frerot, and P. Jouin.** 1991. Oxybenzotriazide free peptide coupling reagents for N-methylated amino acid. Tetrahedron Lett. **32:**1967–1970.
9. **Davis, D. G., B. F. Gisin, and D. C. Tosteson.** 1976. Conformational studies of peptide cyclo-(D-Val-L-Pro-L-Val-D-Pro)$_3$, a cation binding analogue of valinomycin. Biochemistry **15:**768–774.
10. **Genty, B., J. M. Briantais, and N. R. Baker.** 1990. The relationship between the quantum yield of photosynthetic electron transport and quenching of chlorophyll fluorescence. Biotechnol. Biophys. Acta **990:**87–92.
11. **Gerhardstein, B. L., T. Gao, M. Bunemann, T. S. Puri, A. Adair, H. Ma, and M. M. Hosey.** 2000. Proteolytic processing of the C terminus of the alpha(1C) subunit of L-type calcium channels and the role of a proline-rich domain in membrane tethering of proteolytic fragments. J. Biol. Chem. **275:**8556–8563.
12. **Glynn, P. W.** 1991. Coral reef bleaching in the 1980s and possible connections with global warming. Trends Ecol. Evol. **6:**175–179.
13. **Hoegh-Goldberg, O., and B. Salvant.** 1995. Periodic mass-bleaching and elevated sea temperatures: bleaching of outer reef slope communities in Moorea, French Polynesia. Mar. Ecol. Prog. Ser. **121:**181–190.
14. **Kaiser, E., R. L. Colescott, C. D. Bossinger, and P. I. Cook.** 1970. Color test for detection of free terminal amino groups in the solid phase synthesis of peptides. Anal. Biochem. **34:**595–598.
15. **Krause, G. H., and E. Weis.** 1991. Chlorophyll fluorescence and photosynthesis: the basics. Annu. Rev. Plant Physiol. Plant Mol. Biol. **42:**313–349.
16. **Kushmaro, A., E. Rosenberg, M. Fine, Y. Ben-Haim, and Y. Loya.** 1998. Effect of temperature on bleaching of the coral *Oculina patagonica* by *Vibrio* AK1. Mar. Ecol. Prog. Ser. **171:**131–137.
17. **Kushmaro, A., Y. Loya, M. Fine, and E. Rosenberg.** 1996. Bacterial infection and coral bleaching. Nature **380:**396.
18. **Kushmaro, A., E. Rosenberg, M. Fine, and Y. Loya.** 1997. Bleaching of the coral *Oculina patagonica* by *Vibrio* AK-1. Mar. Ecol. Prog. Ser. **147:**159–165.
19. **Madison, V., M. Atreyi, C. M. Deber, and E. R. Blout.** 1974. Cyclic peptides. IX. Conformations of a synthetic ion-binding cyclic peptide, cyclo-(pro-gly)3, from circular dichroism and ^{1}H and ^{13}C nuclear magnetic resonance. J. Am. Chem. Soc. **96:**6725–6734.
20. **Nicolas, P., and A. Mor.** 1995. Peptides as weapons against microorganisms in the chemical defense system of vertebrates. Annu. Rev. Microbiol. **49:**277–304.
21. **Park, C. B., M. S. Kim, and S. C. Kim.** 1996. A novel antimicrobial peptide from *Bufo bufo gargarizans*. Biochem. Biophys. Res. Commun. **218:**408–413.
22. **Park, J. M., J. E. Jung, and B. J. Lee.** 1994. Antimicrobial peptides from the skin of a Korean frog, *Rana rugosa*. Biochem. Biophys. Res. Commun. **205:**948–954.
23. **Schreiber, U., U. Schliwa, and W. Bilger.** 1986. Continuous recording of photochemical and non-photochemical chlorophyll fluorescence quenching with a new type of modulation fluorometer. Photosynth. Res. **10:**51–62.
24. **Schreiber, U., K. Kuhl, I. Lkimant, and H. Reising.** 1996. Measurement of chlorophyll fluorescence within leaves using a modified PAM fluorometer with a fiber-optic microprobe. Photosynth. Res. **47:**103–109.
25. **Schreiber, U., R. Gademann, P. J. Ralph, and A. W. D. Larkum.** 1997. Assessment of photosynthetic performance of *Prochloron* in *Lissoclinum patellae in hospite* by chlorophyll fluorescence measurements. Plant Cell Physiol. **38:**945–951.
26. **Shai, Y.** 1995. Molecular recognition between membrane-spanning polypeptides. Trends Biochem. Sci. **20:**460–464.
27. **Smith, F. A., and J. A. Raven.** 1979. Intercellular pH and its regulation. Annu. Rev. Plant Physiol. **30:**289–311.
28. **Steinauer, R., and P. White.** 1994. Innovations and perspectives in solid phase synthesis, p. 689–692. *In* R. Epton (ed.), 3rd International Symposium. Mayflower Worldwide Ltd., Birmingham, England.
29. **Steiner, H., D. Andreu, and R. B. Merrifield.** 1988. Binding and action of cecropin and cecropin analogues: antibacterial peptides from insects. Biochim. Biophys. Acta **39:**260–266.
30. **Suh, J. Y., Y. T. Lee, C. B. Park, K. H. Lee, S. C. Kim, and B. S. Choi.** 1999. Structural and functional implications of a proline residue in the antimicrobial peptide gaegurin. Eur. J. Biochem. **266:**665–674.
31. **Sundberg, B., D. Campbell, and K. Palmquist.** 1997. Predicting CO_2 gain and photosynthetic light acclimation from fluorescence yield and quenching in cyano-lichens. Planta **201:**138–145.
32. **Toren, A., L. Landau, A. Kushmaro, Y. Loya, and E. Rosenberg.** 1998. Effect of temperature on adhesion of *Vibrio* strain AK-1 to *Oculina patagonica* and on coral bleaching. Appl. Environ. Microbiol. **64:**1379–1384.
33. **Tosteson, M. T., and D. C. Tosteson.** 1981. The sting. Melittin forms channels in lipid bilayers. Biophys. J. **36:**109–116.
34. **Velthuys, B. R.** 1980. Mechanisms of electron flow in photosystem II and towards photosystem I. Annu. Rev. Plant Physiol. **31:**545–567.
35. **Warren, K. S.** 1961. Ammonia toxicity and pH. Nature **195:**47–49.